Available online at www.sciencedirect.com
ScienceDirect
Polymer 48 (2007) 409–416
polymer
www.elsevier.com/locate/polymer

Molecular dynamics simulations to investigate polymer–polymer and polymer–metal oxide interactions☆

B. Prathab [a], V. Subramanian [b], T.M. Aminabhavi [a,*]

[a] *Molecular Modeling Division, Center of Excellence in Polymer Science, Karnatak University, Pavate Nagar, Dharwad 580 003, Karnataka, India*
[b] *Chemical Laboratory, Central Leather Research Institute, Adyar, Chennai 600 020, India*

Received 29 September 2006; received in revised form 3 November 2006; accepted 6 November 2006
Available online 29 November 2006

Abstract

Polymer–polymer interactions in majority of engineering polymers are difficult to measure experimentally, since many polymers are usually insoluble in solvents, have high glass transition temperatures, and are sometimes poorly characterized. Therefore, applying molecular modeling strategies would be helpful in such situations in order to provide useful information, which would be difficult to obtain by other means. Poly(methyl methacrylate), PMMA, is a widely used engineering polymer that exists in a glassy state at room temperature. Therefore, we have selected PMMA to perform the molecular dynamics simulations to investigate its interfacial interaction with many other important polymers such as PAN, PC, PEO, PES, PMS, PU, PVAc, PVDF, PVME and PVP. Small molecular fragments of repeating units of these polymers were chosen for interaction studies, whose polymers and/or their blends with PMMA are used in many engineering applications. The COMPASS force field methodology was used in the present study for oligomers containing up to 10-mers for simulations to compute solubility parameters that are closely agreeable with the experimental data. Molecular dynamics (MD) simulations have also been performed to explore the adsorption behavior of MMA with several metal oxides (Al_2O_3, Fe_2O_3, SiO_2 and TiO_2), since such studies are important in developing polymer composites. Interfacial interactions between MMA and metal oxides have been calculated using the vibrational absorptions in order to identify the functional groups that might interact quite favorably with the PMMA.

Keywords: Methyl methacrylate; Metal oxides; Interaction energy

1. Introduction

Physical mixtures of different types of polymers have been used extensively to produce the commercially important engineering polymers having combinations of properties that are normally not found in a single polymer. In choosing the appropriate blend systems, prediction of individual polymer miscibility aspects is important in view of their widespread industrial applications. In an effort to understand the miscibility/immiscibility behaviors of two different polymers, efforts have been made to employ various theoretical and experimental tools that will help to investigate the intricate problems involved in polymer miscibility [1,2]. Parallel to such studies, an understanding of polymer–non-polymer interfaces, including those of polymers and metals or metal oxides is equally important before one seeks their diverse applications in developing microelectronic devices, flexible interconnections, photovoltaics, microlithography, microfabrication, polymer-lined metal containers for protective food packaging, polymer composites, adhesives, sealants, etc. [3]. The interfaces of polymers with metals/metal oxides are distinctly different from polymer–polymer interfaces due to widely varying interactions. Therefore, a detailed molecular level strategy to understand the physical interactions and solid-state chemical reactions between polymer surface atoms and metal/metal oxide surfaces as well as near-surface atoms is extremely important to understand the macroscopic properties of a variety of chemically bonded

☆ This paper is Center of Excellence in Polymer Science Communication #132.

* Corresponding author. Fax: +91 836 2771275.
E-mail address: aminabhavi@yahoo.com (T.M. Aminabhavi).

0032-3861/$ - see front matter © 2006 Elsevier Ltd. All rights reserved.
doi:10.1016/j.polymer.2006.11.014

multilamellar dielectric and composite materials. In this sense, the classical simulation study on polymer–polymer and polymer–non-polymer interfaces plays a vital role in investigating the miscibility and adhesion characteristics of such systems, which are inherently difficult to study experimentally or for which experimental data are not available; even if some scanty data are available, they are of uncertain quality. Foremost among the difficult and most important systems is the engineering polymers like poly(methyl methacrylate), PMMA, which is a well-known glassy polymer used in a variety of engineering areas from aircraft glazing to lightweight construction systems [4,5]. However, its widespread industrial exploitation prompted us to undertake a detailed MD simulation studies to probe its compatibility behavior and its adhesion characteristics with other polymers as well as metal oxides. In this contribution, PMMA is chosen as a model polymer to probe its interactions with some other important polymers like poly(acrylonitrile), (PAN); polycarbonate, (PC); poly(ethylene oxide), (PEO); poly(ether sulfone), (PES); poly(α-methyl styrene), (PMS); polyurethane, (PU); poly(vinyl acetate), (PVAc); poly(vinylidene fluoride), (PVDF); poly(vinyl methyl ether), (PVME); poly(vinyl pyrrolidone), (PVP) and metal oxides like corundum (Al_2O_3), hematite (Fe_2O_3), silica (SiO_2) and rutile (TiO_2) using MD simulation strategies.

2. Simulation of polymer–polymer interface

Even though theoretical analysis [6–8] based on the corresponding states theory [9,10] and that of Flory equation-of-state thermodynamics [11–13] provided strong foundations to understand the thermodynamics of compatible polymer mixtures, yet theoretical predictions on binary systems are quite complicated because of the lack of availability of relevant parameterization. Therefore, it is important to predict the interactions between surfaces of such polymers at the molecular level with a reasonable degree of accuracy and success using the computer-based MD simulations. However, the basic thermodynamic principles governing the polymer blend compatibility and their applications to other filled polymeric systems require the accurate knowledge of polymer–polymer interaction parameter, which is important in controlling the phase behavior trends in blends [14–16]. Therefore, the prediction of interfacial properties of such polymers depends critically upon the degree of mutual compatibility between the component polymers and hence, much effort has been devoted to find compatible polymer blends for suitable applications [17].

In an effort to pursue further a theoretical understanding on polymer–polymer and polymer–metal oxide interactions, we have undertaken a detailed study of the interactions of PMMA with polymers like PAN, PC, PEO, PES, PMS, PU, PVAc, PVDF, PVME and PVP using the MD simulation protocols. Blends of these polymers have applications in many areas of science and technology including membranes and medicine [18–23]. But, the structural complexity and rigidity of these polymers, due to factors such as molecular packing, chain flexibility and molecular weight [15,24,25] make them complicated in terms of their relaxation modes. It is, therefore, not feasible to perform the full-detailed atomistic MD simulations to obtain macroscopic bulk properties of the polymers. Detailed treatment of the fast modes would slow down the run time so strongly that slow modes cannot reach equilibrium in a reasonable time. In addition, atomistic details sometimes obscure the interesting properties. Dense long chain polymer systems are very difficult to equilibrate using conventional simulation methods [26]. The longest relaxation time of the polymer melts ranges from microseconds (μs) to seconds. However, from the study of oligomers and related small molecules, with extrapolation to high molecular weight [27], one could partially circumvent many of these problems. Hence, in the present investigation, MD simulations of the oligomeric forms of these polymers have been performed successfully at the room temperature.

2.1. Modeling details

Molecular simulations were performed using MS modeling 3.1 software purchased from Accelrys, San Diego, CA, USA [28]. The simulation methodology includes molecular mechanics (MM) and molecular dynamics (MD) calculations using the Discover module [29]. MD was performed using the COMPASS (condensed-phase optimized molecular potentials for atomistic simulation studies) force field [30], which is one of the first ab initio force field approaches that has been parameterized and validated using the condensed-phase properties. The minimization was performed using the steepest descent approach followed by the conjugate gradient method. The temperature in all the simulations was equilibrated with the Andersen algorithm [31]. The velocity Verlet algorithm [32] was then used to integrate the equations of motion. The non-bonded interactions have been calculated using group-based method with explicit atom sums being calculated to 9.5 Å. The tail correction was applied to non-bonded interactions during the MD run.

The oligomer chain was generated with 10 monomer units. It was minimized and amorphous cells were constructed based on the respective densities of the selected oligomers. The method used in constructing the amorphous cell module of MS modeling was the combined use of an algorithm developed by Theodorou and Suter [33] and the scanning method of Meirovitch [34]. Chain conformations were assumed to resemble those of the unperturbed chains that are found with significant probability in the bulk.

Initially, the proposed structure was generated by using the rotational isomeric state (RIS) model of Flory [24], describing the conformations of the unperturbed chains. In order to avoid excessive overlaps between chains, modified conditional probabilities were used, which could account for non-bonded interactions between atoms to be placed and rest of the system. Initial structures were minimized by turning on potential interactions such that more severe overlaps were relaxed first and then gradually, the minimum was reached by switching on the full potential. In the scanning method, all possible continuations of the growing chains were taken into account while computing the conditional probabilities. The constructed

amorphous cells were minimized to a convergence level of 0.01 kcal/mol/Å using the same method as described before.

MD simulations under constant volume and temperature (*NVT*) ensemble were performed using the Discover program. Systems built with 3D periodicity were equilibrated in the *NVT* ensemble at 298 K. Molecular dynamics run for 10 ps have been performed to remove the unfavorable local minima that had high energies. Subsequently, systems are subjected to 200 ps of dynamics with the trajectories being saved every 0.1 ps during the last half of the run to calculate the physical properties of interest.

2.2. MMA-oligomer model

MMA oligomeric slab was constructed using the confined layer (cell type) dialog in the amorphous builder. As a part of the amorphous cell construction, a geometry refinement of the structure was performed. Further, 2D boxes were built using the algorithm as described above, whereupon MMA and the selected oligomer slabs were piled up and the box was extended by 100 Å in the *c*-direction. In order to pile the cells correctly, other oligomeric systems were selected such that they have almost the same base-size by choosing *a* and *b* cell dimensions to be compatible with those of MMA. MD simulations were run in the *NVT* ensemble at 298 K with a tail correction applied outside the cut-off of 9.5 Å. This ensures that a relatively thin layer would feel the effective pressure equivalent to that in the bulk. Because the system contains a vacuum space, both the oligomeric systems are free to expand even though the ensemble is at a constant volume.

The systems were then allowed to equilibrate normally under vacuum for approximately 30,000 steps. This was followed by a 300 ps of MD run. For every 500 fs (femto seconds), the energy of interaction between oligomeric layers was evaluated using 18 Å cut-off distance without the tail correction. The applied cut-off distance gives a consistent and reasonably accurate measure of the total energy of interaction of the two layers. A representative structure of MMA with the oligomer is illustrated in Fig. 1. A total of 600 energy evaluations were performed for each system (300 ps total simulation time). Visual description of the energy evaluation as a function of time is represented in Fig. 2.

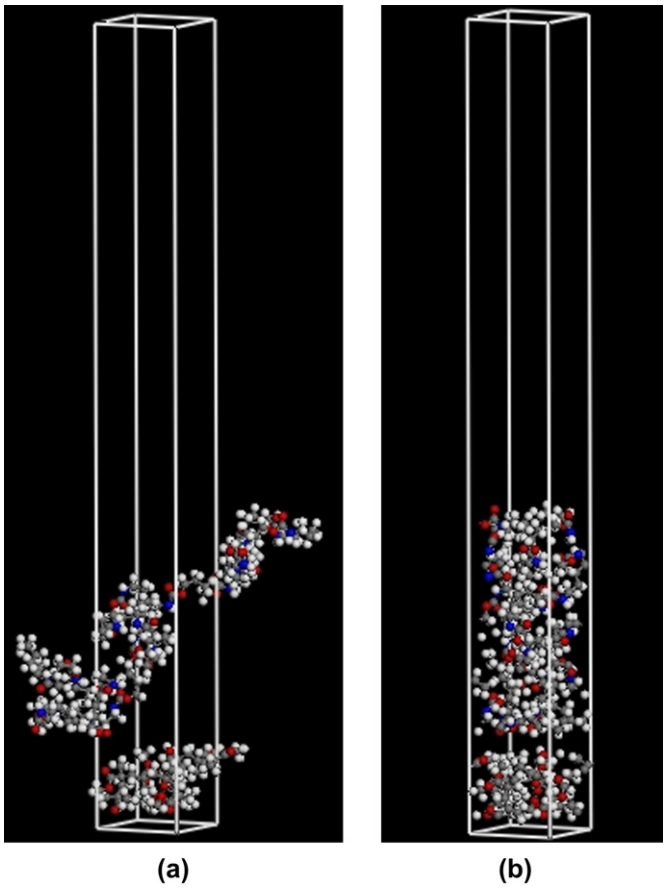

Fig. 1. A representative structure of MMA interacting with urethane. (a) Molecules are superimposed on the cell. (b) Molecules are packed into the cell with their periodic images (colors: carbon atoms—grey, hydrogen—white, oxygen—red, and nitrogen—blue). (For interpretation of the references to color in this figure legend, the reader is referred to the web version of this article.)

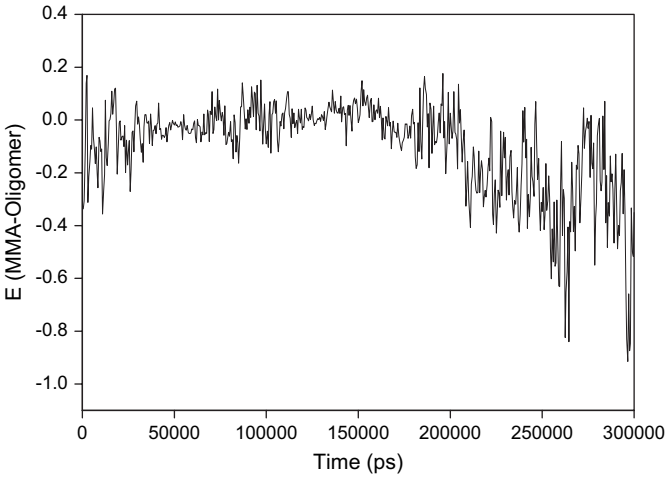

Fig. 2. The energy evaluation of methyl methacrylate with vinyl acetate.

3. Simulation of polymer–non-polymer interface

From the standpoint of adhesion science, it is important to study the interaction between polymer and metal oxide surfaces, since such systems represent a new class of polymeric materials, which combine the properties of embedded inorganic particles (in terms of mechanical strength, modulus, thermal stability, etc.). Efforts in this direction have been made earlier on the encapsulation of calcium carbonate [35], barium sulfate [36] and colloidal silica [37] using a variety of polymers including PMMA, polystyrene [38], poly(vinyl acetate) and polypyrrole [39]. In recent times, computational efforts have been made to investigate polymer–non-polymer interfaces [40,41]. However, to the best of our knowledge, theoretical simulations that incorporate the role of metal-oxide surfaces with PMMA have not been published in the earlier literature. Hence, our approach to investigate the interactions of oligomers with metal-oxide surfaces will be of great significance because such computations will be a pre-requisite to extend the

more detailed molecular simulations of long chain polymers near the surfaces where chemisorptions could occur. Here, the related quantity of interest is the energy of adhesion, which is the energy released when two bodies of different surfaces are brought in contact with each other. The strength of adhesion holding the two materials together is a function of attractive or retaining forces at the interface between them. In this context, we have chosen MMA oligomer to study its adhesion behavior with metal oxides such as Al_2O_3, Fe_2O_3, SiO_2 and TiO_2.

3.1. Oligomer

Oligomer generation and construction of simulation cell followed the same methodology as described in Section 2.1. However, cell dimensions are taken in such a way that *a* and *b* (crystal) lattice parameters for the oligomer remained the same as *u* and *v* (surface) parameters for metal oxide surface.

3.2. Metal oxides

The unit cell structure of metal oxides was available with the MS modeling (Accelrys). Since these are the experimentally determined crystal structures, the lattice parameters are indeed the experimental parameters. In order to substantiate the applicability of COMPASS force field to study the properties of metal oxide structures, we have compared the experimental lattice parameters, *a* and *c*, and internal oxygen positional parameters, *u*, of the metal oxides (TiO_2) with those of the minimized crystal structure predicted by COMPASS force field. The lattice parameter values of $a = 4.594$ Å and $c = 2.959$ Å were used for the crystal structure of TiO_2. By selecting the oxygen atom at position (*u*, *u*, 0), the coordinates of oxygen atom were found to be (0.30479974, 0.30479974, 0). However, for optimizing the metal oxides, atom typing was necessary, which sets the correct force field parameter to be used in determining the energies and forces for the system. Usually, the Discover module in MS performed atom typing automatically, but in the case of metal oxides, they were typed manually with the typing engine in the Discover. As the bonds between metal and oxygen atoms are ionic in nature, the parameters do not exist for covalent bonds between them and hence, the bonds must be removed for minimization to proceed. Otherwise, the Discover will look for bond parameters, which do not exist.

Discover minimizer was then used to optimize the structure and after the minimization, the lattice parameters *a* and *c*, and the *u* coordinate of the oxygen atom were noted down. The values of *a*, *c* and *u* are 4.594, 2.959 and 0.30243540, respectively, which compared well with the experimental data [42]. Using the surface builder module of MS modeling, metal oxide surfaces were prepared by employing the desired cleave planes (*hkl*), which provided the fractional depth of the surface that should be more than the non-bonded cut-off distance of 9.5 Å. The relaxation of metal oxide surface followed the same procedure as discussed before. Crystal surface of the metal oxide slab to be used in the simulation box to study the adhesion calculation was built by utilizing the crystal builder facility in MS modeling.

3.3. Polymer–metal oxides

The oligomer (MMA) was assembled in the simulation box with the metal oxide surface and *c*-dimension of the box was extended to 30 Å, such that the oligomer was at an equi-distance from the metal oxide surface and it can see only one side of the surface. The MD simulation was then performed for 300,000 steps with a time step of 1 fs at 298 K. As the metal oxide surface was minimized in the earlier step, the entire surface atoms were constrained during *NVT* dynamics. The simulated structure of MMA with metal oxides is depicted in Fig. 3.

Energy of adhesion was calculated according to Eq. (1). At first, the energy (E_{total}) for the simulation box containing both MMA and surface atoms was calculated and then, the energy of oligomer (E_{MMA}) was calculated without any contribution from the surface. Finally, the surface atoms were kept and MMA was removed to calculate the energy of the surface ($E_{surface}$). The energy of adhesion of MMA and the surface was then computed as:

$$E_{adhesion} = \frac{E_{total} - \left(E_{surface} + E_{MMA}\right)}{V} \quad (1)$$

where *V* is the molar volume of MMA.

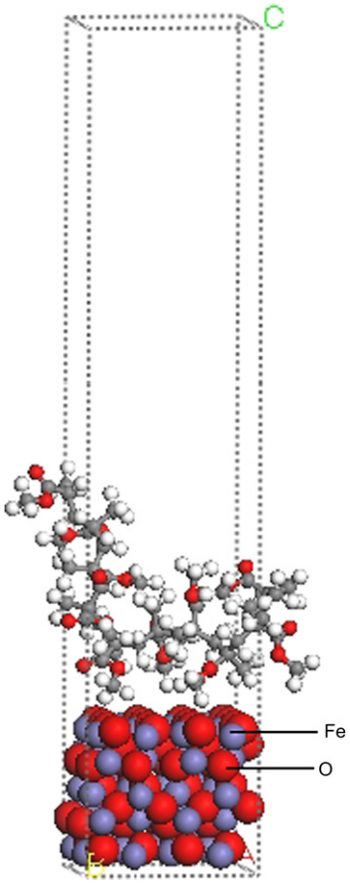

Fig. 3. A typical simulated MMA and its interface with Fe_2O_3 surface (colors: carbon atoms—grey, hydrogen—white, and oxygen—red). (For interpretation of the references to color in this figure legend, the reader is referred to the web version of this article.)

4. Results and discussion

4.1. Interaction of MMA with oligomers

Cohesive properties of the polymers are difficult to determine experimentally because the chosen polymers are insoluble, have high glass transition temperatures and are sometimes poorly characterized. Therefore, we thought of employing the MD simulations, which will provide useful information of higher quality than other methods. We have therefore performed series of MD simulations to calculate the cohesive energy density (CED) of these polymers. In order to validate the simulation protocols using COMPASS force field, solubility parameters of these polymers have been calculated from CED data using Eq. (3) [43].

In molecular simulation studies on polymers, cohesive energy, E_{coh} is defined as the increase in energy per mole of a polymer if all intermolecular forces are eliminated. On the other hand, CED corresponds to cohesive energy per unit volume. If V_{mol} is molar volume of the polymer, then CED is defined as

$$\mathrm{CED} = (E_{coh}/V_{mol}) \quad (2)$$

CED is related to Hildebrand solubility parameter, δ through the equation:

$$\delta = (E_{coh}/V_{mol})^{1/2} \quad (3)$$

In this context, the computed δ value of 9.62 $(\mathrm{cal/cm^3})^{1/2}$ for MMA compared well with the literature value of 9.45 $(\mathrm{cal/cm^3})^{1/2}$. The solubility parameter of oligomers used in these studies and their interaction energies with MMA surface model are given in Table 1. It is observed that δ values agreed well with the literature data [44] within the limits of experimental errors, but higher deviations are observed for vinyl pyrrolidone, since the experimental data for this system are highly scattered. It is evident that there is a good agreement between the calculated and experimental δ values, suggesting that molecular simulation strategies adopted in this investigation provide the reliable estimates of solubility parameters of polymers.

Interfacial interaction energies of the nine chosen oligomers shown in the fifth column of Table 1 reveal their compatibility range with MMA. Notice that the average interaction energies of vinylidene fluoride, vinyl methyl ether, vinyl acetate, vinyl pyrrolidone and ethylene oxide have shown negativity, indicating that these systems are miscible with MMA. Further, systems like vinylidene fluoride, vinyl methyl ether and vinyl acetate exhibited a better compatibility as ascertained from their interaction energy values. However, in the case of oligomers like urethanes and carbonates, the miscibility range decreased systematically (see Table 1). Besides, the interaction energy of α-methyl styrene, urethane and carbonate, accentuates their partial miscibility with MMA. A profound incompatible behavior was seen with ether sulfone and acrylonitrile. Hence, the present study reveals the compatibility of MMA and its miscibility with the selected oligomers of this study. In order to substantiate our computational results, we have included the experimental observations of miscibility/immiscibility characteristics of the aforementioned polymer pairs in Table 1. It is noticed that the computed interaction energies of MMA with the chosen oligomers are in accordance with the experimental observations.

4.2. Interaction of MMA with metal oxides

Computation of interaction energy of metal oxides is important to understand the physisorption of metal oxides with MMA. The surface construction of metal oxide is an important step in the calculation of interaction energy [54,55]. In this study, quartz crystalline structure of SiO_2, with a trigonal symmetry, was considered. The main crystal forms are rhombohedrons (101), (011) (with similar surface structure) and hexagonal prism (100). Of these planes, the (100) plane of silica exhibits a marked adhesion property since (100) face of quartz SiO_2 contains abundant number of surface sites [56]. Hence, for SiO_2, the largest face of the crystal was the (100) surface and therefore, it was used as a surface against which MMA was brought in contact during the simulation step. Generally, the surfaces expressed in rutile were (011), (110), (100) and (221) with surface energies of 1.85, 1.78, 2.08 and 2.02 $\mathrm{Jm^2}$, respectively.

Table 1
Densities and solubility parameters of oligomers and their interaction energies with methyl methacrylate

Oligomers (10-mers)	Density ($\mathrm{g/cm^3}$)	Solubility parameter $(\mathrm{cal/cm^3})^{1/2}$		Interaction energy ($\mathrm{cal/cm^3}$)	Experimental observation
		δ (simulated)	δ (literature) [44]		
Vinylidene fluoride	1.75	9.34 (0.35)	9.38	−0.166 (0.376)	Miscible [45]
Vinyl methyl ether	1.03	9.47 (0.13)	9.61	−0.112 (0.122)	Miscible [46]
Vinyl acetate	1.19	8.95 (0.18)	8.90	−0.098 (0.173)	Miscible [47]
Ethylene oxide	1.30	9.82 (0.36)	9.73	−0.031 (0.147)	Miscible [48]
Vinyl pyrrolidone	1.04	10.04 (0.20)	11.06	−0.024 (0.235)	Miscible [49]
1-Methyl styrene	1.07	9.31 (0.22)	9.45	0.003 (0.107)	Partially miscible [17]
Urethane	1.07	9.43 (0.13)	9.80	0.010 (0.662)	Partially miscible [50]
Carbonate	1.20	9.73 (0.16)	9.92	0.043 (0.214)	Partially miscible [51]
Ether sulfone	1.24	9.75 (0.30)	9.90	0.122 (0.326)	Immiscible [52]
Acrylonitrile	1.18	12.36 (0.26)	12.35	0.131 (0.199)	Immiscible [53]

Values in the parentheses indicate (±) standard deviations.

In general, adhesion increases with decrease in surface energy. It should also be noted that there is a direct correspondence between the concepts of 'surface stability' and 'surface energy', i.e., surfaces with lower surface energy will be more stable and vice versa. Hence, the most stable surface of rutile being (110), which is certain from its surface energy values. Further, TiO_2 (110) surface is characterized by rows of bridging oxygen atoms that are running along the (110) direction [57]. This surface also exposes Ti atoms not capped by the oxygen atoms, in rows parallel to the bridging oxygen's; therefore, they are expected to expose the dangling bonds at the surface to create a high adhesion. Hence, the surface plane for TiO_2 was (110), which is apparent from the above discussion.

Hematite (Fe_2O_3) and corundum (Al_2O_3) possess trigonal symmetry. The main crystal forms of Fe_2O_3 and Al_2O_3 are basal pinacoid (001), sharp (101) and nearly isometric (012) rhombohedrons. However, (001) and (012) of hematite and corundum are the widely studied surfaces. Also, the sequence of Fe_2O_3 and Al_2O_3 follows similar stacking arrangement. The surface energy values of (001) surface of Fe_2O_3 and Al_2O_3 are found to be 4.24 and 3.77 J/m^2, respectively. Similarly, for (012) surface, the surface energy values are found to be 2.79 and 2.95 J/m^2, respectively [58]. As mentioned earlier, the surface energy of (012) surface is low when compared to (001) surface. Thus, from the above discussion, it is apparent that (012) is the most prevalent and stable surface for both hematite and corundum [59].

In PMMA, the primary site of interaction with metal/metal oxide surface is C═O and C−O groups [60]. It was presumed that the intensity ratio of C−O−C bond decreases when compared to C═O bond. This may be due to the cleavage of methoxy group of PMMA upon interaction with metal oxide surface. The intensity calculation by simulation approach will be discussed later. In the following, the resulting orientation and energy of MMA adsorbed on four different metal oxide surfaces are compared with each other. Fig. 4(b) shows the end configuration of MMA at the corundum (Al_2O_3) surface obtained from the starting configuration shown in Fig. 4(a). The configurations are typical examples out of about 20 simulations with a wide variety of different starting configurations. Most of the runs ended up with configurations similar to Fig. 4(b) from the inspection of snapshots of the end configuration.

A similar configuration was observed for MMA with other metal oxide surfaces, but not displayed here to avoid redundancy. Therefore, the conclusion can be drawn that a distinct type of conformation was observed for MMA, i.e., the tail like methoxy group is attached to the surface. In the case of Fe_2O_3, the energy necessary to separate segments of MMA from hematite (i.e., the adhesive energy value) was calculated to be −251.82 cal/cm^3. Similarly, for Al_2O_3, the energy was found to be −187.06 cal/cm^3. Further, for SiO_2 and TiO_2, the calculated adhesive energies are −148.50 and −98.99 cal/cm^3, respectively. It is noticed that in the case of hematite, the interaction energy is significantly greater than other metal oxides; nevertheless, corundum and silica exhibited preferential adhesiveness, which is certain from its adhesion energy value. The interaction energy value of rutile is modest than those found for other metal oxide surfaces, indicating their lesser adherence with MMA.

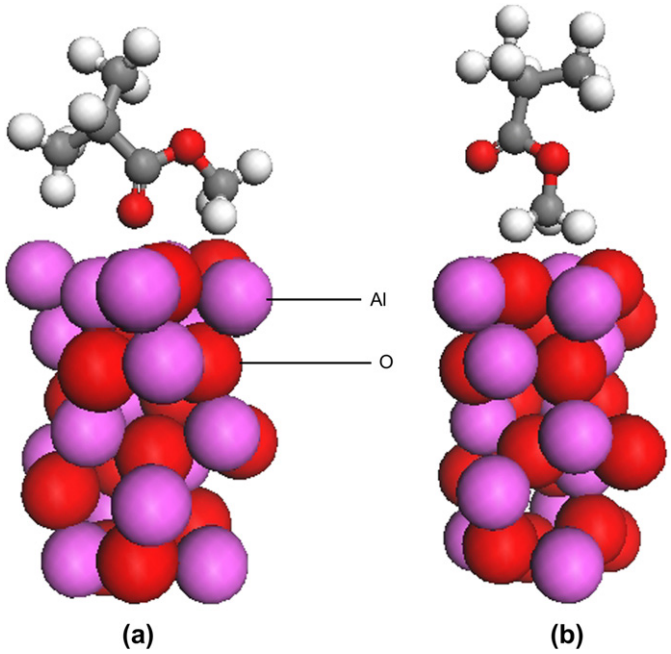

Fig. 4. Starting and end configurations of an adsorbed MMA on Al_2O_3 surface.

In order to demonstrate the adhesive nature of MMA with metal oxides, we have characterized the interaction of these metal oxides with MMA through computations of intensity of vibrational absorptions. In the past, vibrational characterization of interaction of metal oxides with polymers has been determined experimentally [61]. In the present investigation, theoretical simulations of such interactions were calculated through intensity of vibrational absorptions. In this contribution, we have computed the vibrational intensity of MMA with chosen metal oxides through instantaneous normal-mode analysis (INMA) [62,63]. The vibrational intensity was calculated by employing the Discover package. As the force constants are well defined, the vibrational absorptions can be calculated with a good accuracy. Taking this into consideration, we have examined the interaction between metal oxide and the C−O group of PMMA from the intensities of vibrational modes. This tendency is characterized by calculating the intensity and vibrational modes of C−O−C bond of MMA by INMA method. In the usual experimental approach, the mode compositions of bands observed in vibrational spectra are characterized by considering a series of isotope substitutions. Thus, by INMA method, Hessian matrices derive all the isotopic effects at a negligible computational effort. Furthermore, the Hessians' yield normal modes, which allow for straightforward analyses of mode compositions. In this regard, we have minimized MMA by selecting several snapshots at temporal distance of 30 ps and have determined the corresponding Hessian, normal modes and IR intensities.

From the spectroscopic data [64] of PMMA, vibrational modes of C═O and C−O−C are measured to be in the range of 1700−1750 cm^{-1} and 1100−1200 cm^{-1}, respectively. The simulated vibrational modes of C═O and C−O−C are 1805

Table 2
Vibrational frequencies and intensities for the chosen metal oxides and MMA interfaces

Oligomer/metal oxide interface	Frequency of C–O–C (cm^{-1})	Intensity (km/mol)
MMA/Fe_2O_3	1193	0.808
MMA/Al_2O_3	1155	1.237
MMA/SiO_2	1132	1.827
MMA/TiO_2	1120	2.159

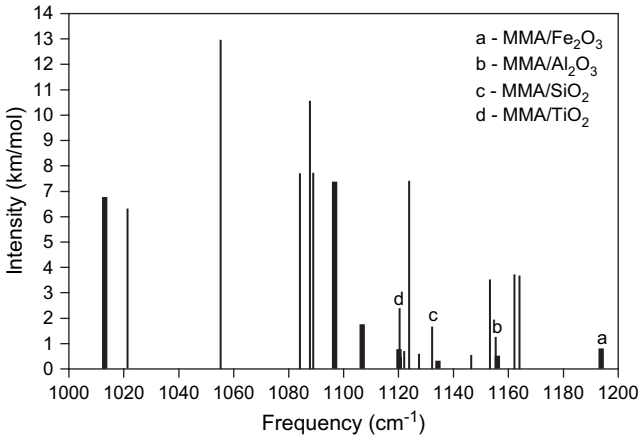

Fig. 5. Plot of IR intensity as a function of frequency.

and 1211 cm^{-1}, respectively, with the intensity of 40.04 and 3.78 km/mol. The simulated frequencies and their intensities for MMA/Fe_2O_3, MMA/Al_2O_3, MMA/SiO_2 and MMA/TiO_2 interfaces are given in Table 2, indicating a decrease in trend of the intensities of C–O–C bond as compared to C–O–C bond intensity of MMA. The predicted IR intensities for the above-mentioned interfaces are plotted as a function of frequency in Fig. 5. In order to compare the intensities of C–O–C bond of the chosen metal oxides, we have scaled down the vibrational frequencies from 1000 to 1200 cm^{-1}. Thus, it is clear that the intensity of C–O–C bond weakens upon interaction with metal oxides; it also follows that intensity increases in an order for metal oxides having less preference for interaction with MMA. Further, the intensity observed for C–O–C bond in MMA/Fe_2O_3 is lower when compared to MMA/Al_2O_3 and in the case of MMA/SiO_2, the intensity is more in contrast to MMA/TiO_2. Thus, the above observation clearly suggests the preferred interaction/adherence of Fe_2O_3 particles with MMA followed by Al_2O_3 and then, SiO_2 and TiO_2 particles. Therefore, the calculation of adhesive character of the aforementioned metal oxides with MMA through the intensity ratio of C–O–C bond by the vibrational modes provides reliable estimates with the observed interaction energies.

5. Conclusions

Molecular modeling approach employed in this research provides a good insight into the polymer–polymer and polymer–non-polymer interfacial interactions. Models of interfaces of methyl methacrylate in interaction with a variety of low molecular weight oligomers of other polymers having a range of solubility parameters show that relatively simple determination of molecular interaction energies studied here will suffice to identify the molecules that can interact favorably with PMMA surface. Also, the negative values of interaction energy should be anticipated whenever strong hydrogen-bonding or acid–base interactions exist. When interaction energy shows increasing negative values, mutual solubility of the polymer pair increases. These interaction studies using MD simulation protocols have been used to explain the phase equilibrium behavior of polymer–polymer systems. Calculations of δ for the chosen systems using the COMPASS force field approach compared well with the literature data, suggesting the validity of the proposed method. However, the interfacial study of MMA and metal oxides involves the determination of adhesion of MMA with four metal oxides (Fe_2O_3, Al_2O_3, SiO_2 and TiO_2).

The chosen crystal faces of the aforementioned metal oxides are shown to be correct, which is obvious from their surface energy values. The present calculations clearly demonstrate a better adhesion between MMA oligomer and all the metal oxides studied. Furthermore, the simulation of vibrational spectra of MMA and the adsorbed MMA onto metal oxides revealed that there is a decrease in the intensity of C–O–C bond in the case of adsorbed MMA. Moreover, the intensity ratio of C–O–C bond of MMA/Fe_2O_3, MMA/Al_2O_3, MMA/SiO_2 and MMA/TiO_2 is in excellent agreement with the calculated values of interaction energies of metal oxides with MMA. The present approach therefore, successfully offers new insights on the influence of functional group (C–O) on the adsorption of PMMA. It also contributes to a better fundamental understanding of the complicated physical interfacial process. The evaluation of interfacial chemistry between various metal oxides and polymers will provide a basis for the design and synthesis of nanoclusters. The future extension of this research is envisaged to other metal oxide surfaces as well as models comprising other polymers. However, further data and analysis are needed to develop a more generalized picture of the factors influencing the conformations of macromolecules reacting to form strong bonds with the surfaces.

Acknowledgments

Professor T.M. Aminabhavi and Mr. B. Prathab thank University Grants Commission, New Delhi (Grant No. F1-41/2001/CPP-II) for financial support to establish Molecular Modeling Division at Center of Excellence in Polymer Science (CEPS). This work is a collaborative effort between CEPS, Dharwad and CLRI, Chennai under the MoU. The authors thank Dr. M. Mori, Accelrys, Japan and Mr. R. Parthasarathi, Senior Research Fellow, CLRI for helpful discussions.

References

[1] Zhang M, Choi P, Sundararaj U. Polymer 2003;44:1979.
[2] Jawalkar SS, Adoor SG, Sairam M, Nadagouda NN, Aminabhavi TM. J Phys Chem B 2004;109:15611.
[3] Kickelbick G. Prog Polym Sci 2003;28:83.

[4] Studer V, Pépin A, Chen Y, Ajdari A. Microelectron Eng 2002;61–62:915.
[5] Pérez JPH, Cabarcos EL, Ruiz BL. Biomol Eng 2006;23:233.
[6] Patterson D, Robard A. Macromolecules 1978;11:690.
[7] McMaster LP. Macromolecules 1973;6:760.
[8] Liu DD, Prausnitz JM. Macromolecules 1979;12:454.
[9] Patterson D. Macromolecules 1969;2:672.
[10] Patterson D. J Polym Sci Part C 1968;16:3379.
[11] Flory PJ. J Am Chem Soc 1965;87:1833.
[12] Eichinger BE, Flory PJ. Trans Faraday Soc 1968;64:2035.
[13] Flory PJ. Discuss Faraday Soc 1970;49:7.
[14] Paul DR, Walsh DJ, Higgins JS. Polymer blends and mixtures. In: NATO ASI series E, applied science, no. 89. Dordrecht, The Netherlands: Martinus Nijhoff Publishers; 1985. p. 1.
[15] Olabisi O, Robenson LM, Shaw MT. Polymer–polymer miscibility. New York: Academic Press; 1979.
[16] Freitag D, Grigo U, Muller PR, Nouvertne W. In: Mark HF, Bikales NM, Overberger CG, Menges G, editors. Encyclopedia of polymer science and engineering. 2nd ed. New York: John Wiley; 1988.
[17] Paul DR, Newman S. Polymer blends, vols. I and II. New York: Academic Press; 1978.
[18] Vasile C, Kulshreshtha AK. Handbook of polymer blends and composites, vol. 4. England: Rapra Technology Limited; 2003.
[19] Okumus E, Gurkan T, Yilmaz L. J Membr Sci 2003;23:223.
[20] Krishnan J. J Controlled Release 2002;79:71.
[21] Chiriac AP, Simionescu CI. Polym Test 1997;16:185.
[22] Paine AJ, Luymes W, Mcnulty J. Macromolecules 1990;23:3104.
[23] Schierholz JM, Steinhauser H, Rump AFE, Berkels R, Pulverer G. Biomaterials 1997;18:839.
[24] Flory PJ. Principles of polymer chemistry. Ithaca, New York: Cornell University Press; 1953.
[25] Hildebrand JH, Scott RL. The solubility of non-elecrolytes. New York: Dover; 1964.
[26] Mavrantzas VG, Boone TD, Zervoupoulou E. Macromolecules 1999;32:5072.
[27] Rigby D, Sun H, Eichinger BE. Polym Int 1997;44:311.
[28] Accelrys Inc. MS modeling. San Diego, CA: Accelrys Inc.; 2003.
[29] Lippa KA, Sander LC, Mountain RD. Anal Chem 2005;24:7852.
[30] Sun H. J Phys Chem B 1998;102:7338.
[31] Andersen HC. J Chem Phys 1980;72:2384.
[32] Verlet L. Phys Rev 1967;159:98.
[33] Theodorou DN, Suter UW. Macromolecules 1985;18:1467.
[34] Meirovitch HJ. J Chem Phys 1983;79:502.
[35] Yang Y, Kong XZ, Kan CY, Sun CG. Polym Adv Technol 1999;10:54.
[36] Hasegawa M, Arai K, Saito S. J Polym Sci Part A Polym Chem 1987;25:3117.
[37] Hergeth WD, Steinau UJ, Bittrich HJ, Simon G, Schmutzler K. Polymer 1989;30:254.
[38] Sondi I, Fedynyshyn TH, Sinta R, Matijevic E. Langmuir 2000;16:9031.
[39] Percy MJ, Barthet C, Lobb JC, Khan MA, Lascelles SF, Vamvakaki M, et al. Langmuir 2000;16:6913.
[40] Gee RH, Maxwell RS, Balazs B. Polymer 2004;45:3885.
[41] Katti KS, Sikdar D, Katti DR, Ghosh Pijush, Verma D. Polymer 2006;47:403.
[42] Abrahams SC, Bernstein JL. J Chem Phys 1971;55:3206.
[43] Bicerano J. Prediction of polymer properties. New York: Marcel Dekker; 1993.
[44] Brandrup J, Immergut EH. Polymer handbook. 2nd ed. New York: Wiley Interscience; 1975.
[45] Nishi T, Wang TT. Macromolecules 1975;8:909.
[46] Choi HW, Moon YJ, Jung BJ, Kim CK. Polymer (Korea) 2002;26:245.
[47] Crispim EG, Schuquel ITA, Rubira AF, Muniz EC. Polymer 2000;41:933.
[48] Liu J, Sakai VG, Maranas JK. Macromolecules 2006;39:2866.
[49] da Silva EP, Tavares MIB. Polym Bull 1998;41:307.
[50] Sudhakar K, Singh RP. Rheol Acta 1987;26:560.
[51] Gardlund ZG. In: Han CD, editor. Polymer blends and composites in multiphase systems. Advances in chemistry series no. 206. Washington, DC: American Chemical Society; 1984.
[52] Kim JH, Whang MS, Kim CK. Macromolecules 2004;37:2287.
[53] Utracki LA. Polymer alloys and blends: thermodynamics and rheology. New York: Hanser Publishers; 1990.
[54] Cooper TG, de Leeuw NH. Langmuir 2004;20:3984.
[55] Tasker PW. J Phys C Solid State Phys 1979;12:4977.
[56] Pivovarov S. Encyclopedia of surface and colloid science. New York: Marcel Dekker; 2002.
[57] Zschack P, Cohen JB, Chung YW. Surf Sci 1992;262:395.
[58] Manassidis A, Vita D, Gillan MJ. Surf Sci Lett 1993;285:L517.
[59] Henrich V, Cox PA. Surface science of metal oxides. Cambridge: Cambridge University Press; 1994.
[60] Tannenbaum R, Hakanson C, Zeno A, Tirell M. Langmuir 2002;18:5592.
[61] Konstadinidis K, Thakkar B, Chakraborty A, Potts LW, Tannenbaum R, Tirell M. Langmuir 1992;8:1307.
[62] Nonella M, Mathias G, Tavan P. J Phys Chem A 2003;107:8638.
[63] Cui Q, Karplus M. J Chem Phys 2000;112:1133.
[64] Banwell CN. Fundamentals of molecular spectroscopy. 3rd ed. England: McGraw Hill; 1983.